NanoSIMS multi-element imaging reveals internalisation and nucleolar targeting for a highly-charged polynuclear platinum compound

NanoSIMS dual-element imaging reveals internalization and nucleolar targeting for a highly-charged polynuclear platinum compound.

Louise E. Wedlock,[a,b] Matt R. Kilburn,[b] Rong Liu,[b] Jeremy A. Shaw,[b] Susan J. Berners-Price[*a,c] and Nicholas P. Farrell[*d,a]

Electronic Supplementary Information (ESI†)

CONTENTS

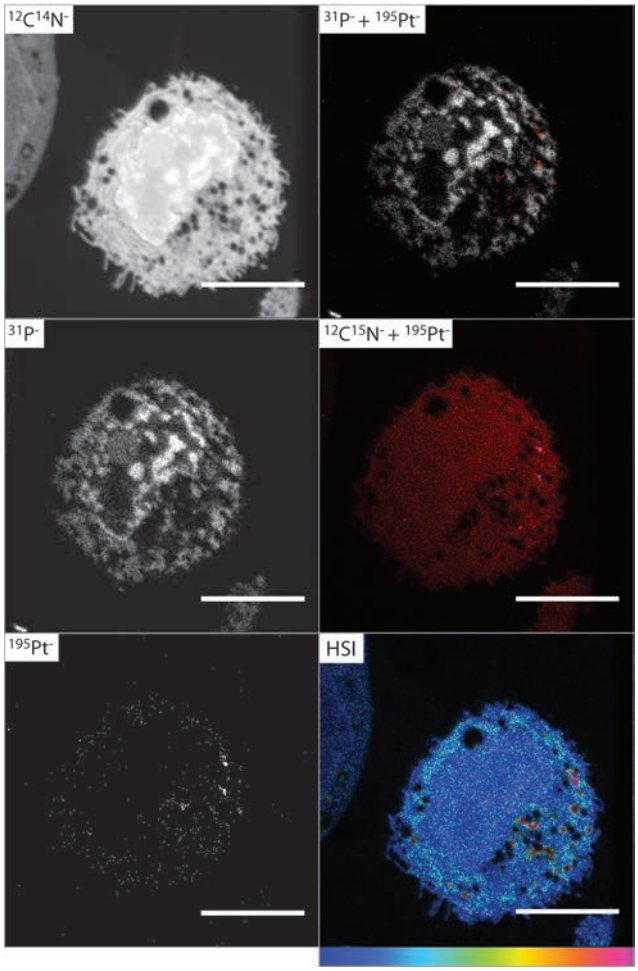

Fig. S1 NanoSIMS secondary ion maps of fixed sections of an MCF7 cell treated with TriplatinNC (20 µM, 1 h). HSI is the hue-saturation-intensity image of the $^{12}C^{15}N^-/^{12}C^{14}N^-$ ratio. A different cell treated under the same conditions is shown in Fig. 1; scale bars = 5 µm.

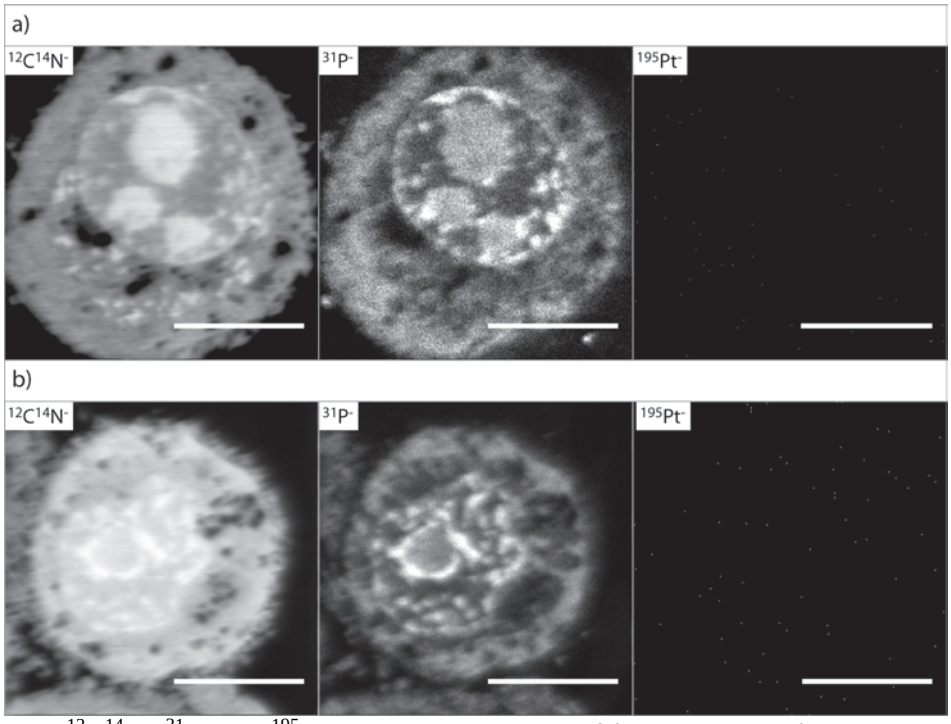

Fig. S2 NanoSIMS $^{12}C^{14}N^-$, $^{31}P^-$, and $^{195}Pt^-$ secondary ion maps of fixed sections of two untreated MCF7 (control) cells (a and b); scale bars = 5 µm. As expected, no Pt signal is observed from the cells.

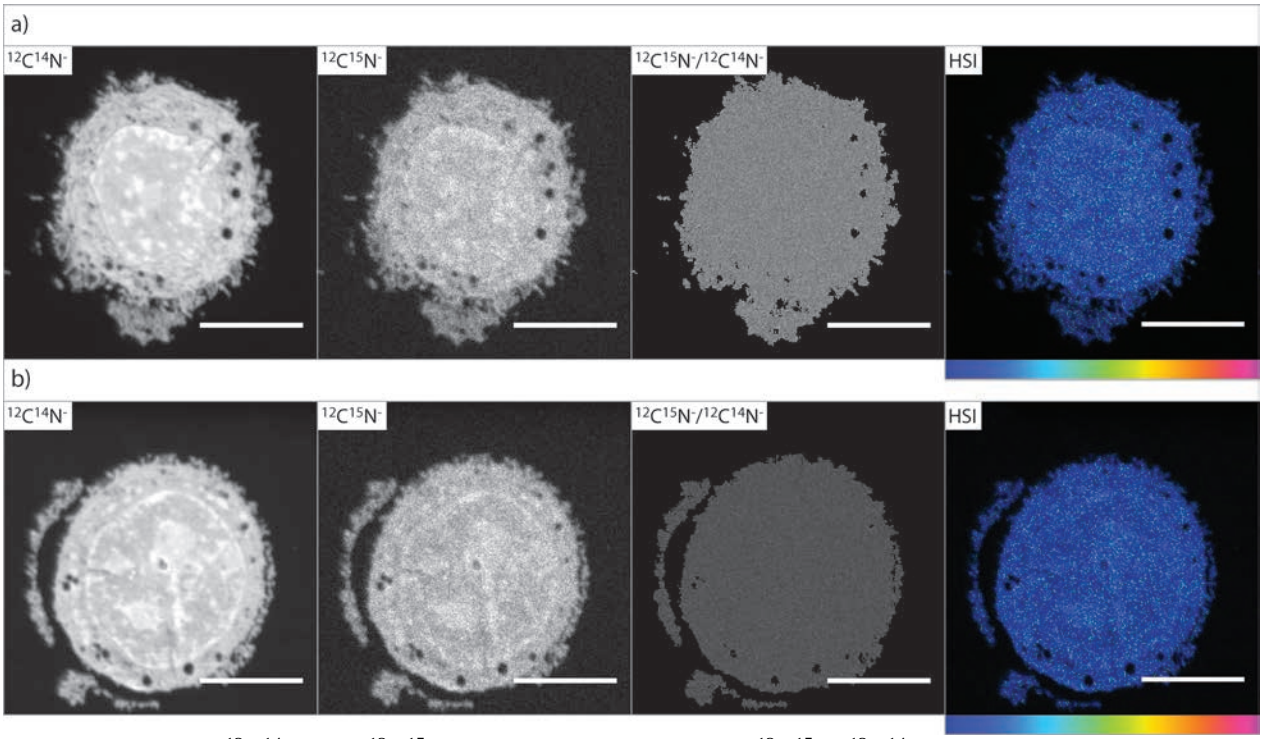

Fig. S3 NanoSIMS $^{12}C^{14}N^-$ and $^{12}C^{15}N^-$ secondary ion maps, the $^{12}C^{15}N^-/^{12}C^{14}N^-$ ratio map and HSI image of two untreated MCF7 cells (a and b); scale bars = 5 µm. No ^{15}N enrichment is observed in the cells.

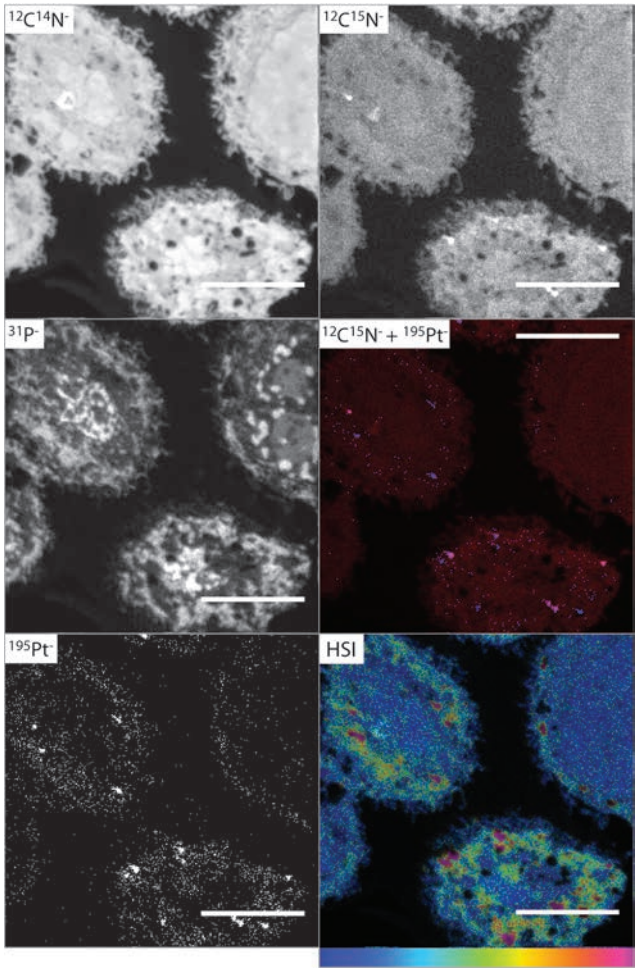

Fig. S4 NanoSIMS secondary ion maps of fixed sections of an MCF7 cell treated with TriplatinNC (20 µM, 2 h). A different cell treated under the same conditions is shown in Fig. 2; scale bars = 5 µm

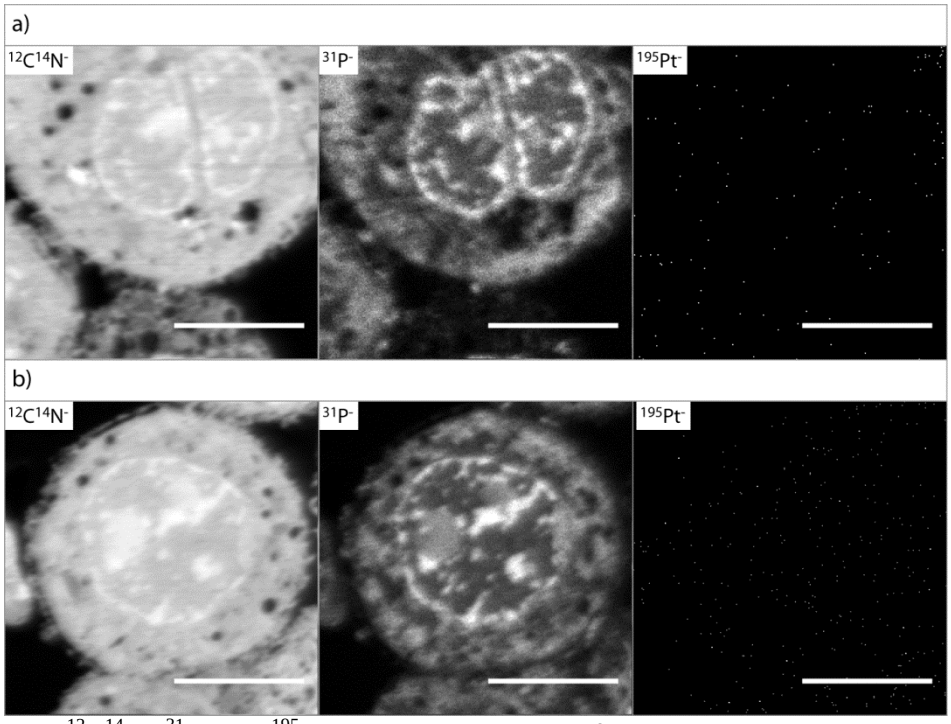

Fig. S5 NanoSIMS $^{12}C^{14}N^-$, $^{31}P^-$, and $^{195}Pt^-$ secondary ion maps of two MCF7 cells (a and b) treated with ^{15}N-labelled cisplatin (20 µM, 1 h); scale bars = 5 µm.

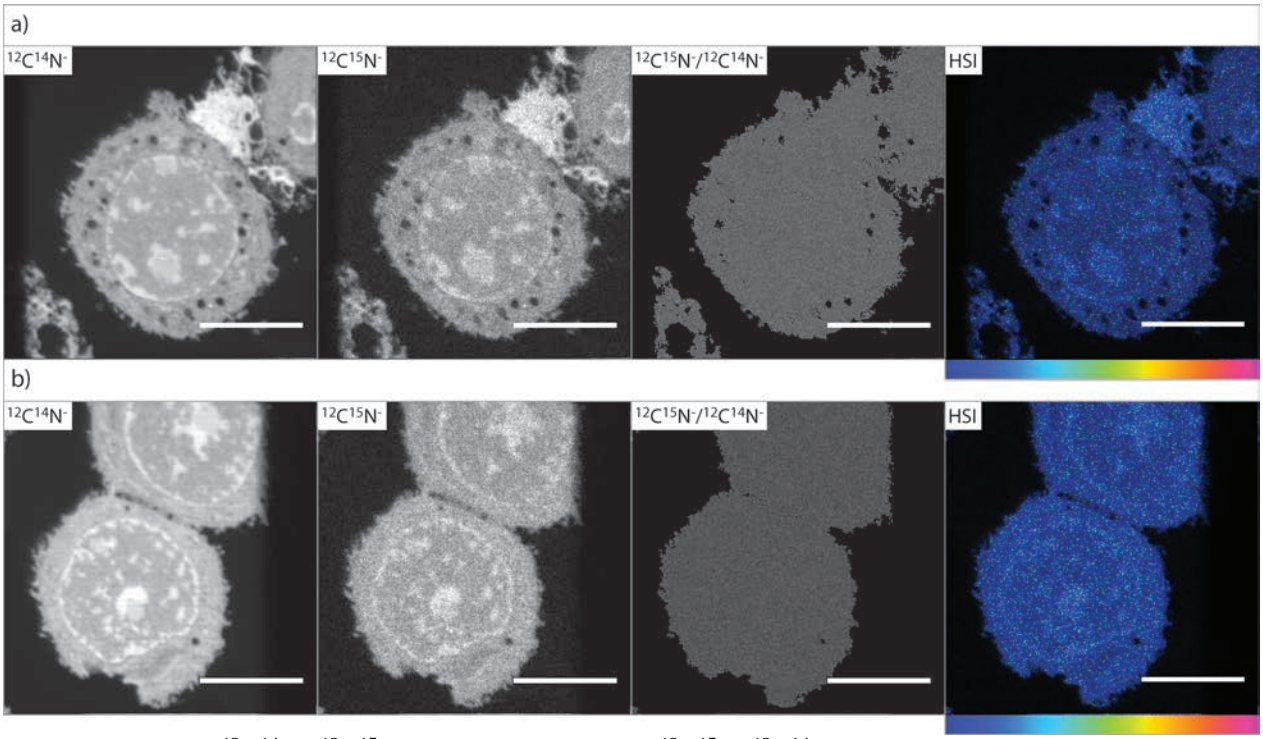

Fig. S6 NanoSIMS $^{12}C^{14}N^-$, $^{12}C^{15}N^-$ secondary ion maps, $^{12}C^{15}N^-/^{12}C^{14}N^-$ ratio maps and HSI images of two MCF7 cells (a and b) treated with ^{15}N-labelled cisplatin (20 µM, 1 h); scale bars = 5 µm. The ratio and HSI images indicate no enrichment in ^{15}N.

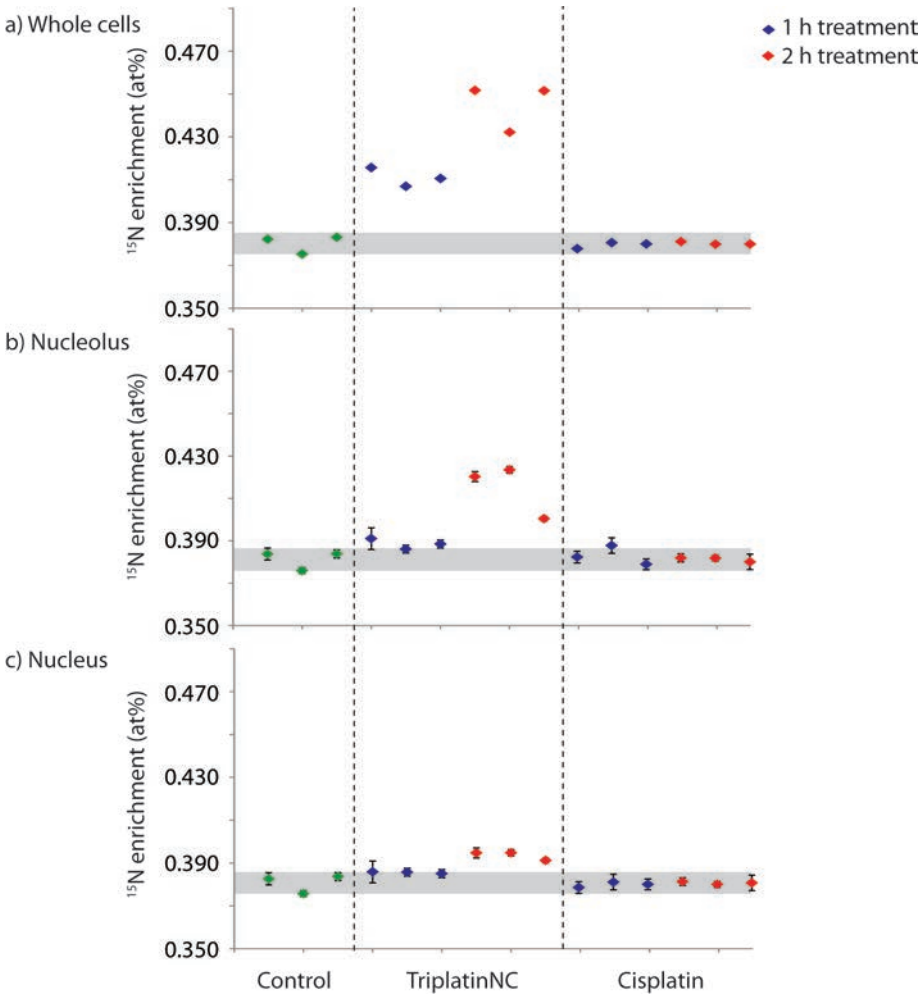

Fig. S7 ^{15}N enrichment (at %) in a) the whole cells; and b) the nucleoli, and c) the nuclei at different exposure times, where data was extracted from at least 3 separate images (see Tables S1, S2 and S3); error bars are expressed as the analytical error on an individual measurement (see text); the grey bars represent the mean of the data obtained from the control samples ± 2 S.E; cells treated with cisplatin showed no enrichment after 2 h, as all values lie within the standard error of the control cells.

Table S1. $^{15}N/^{14}N$ ratio and ^{15}N enrichment data extracted from at least three separate secondary ion images for each treatment, for the whole cells.

Treatment	$^{12}C^{14}N^-$	$^{12}C^{15}N^-$	Ratio	Rel. error (%)	^{15}N (at%)	+/-
Control	364592132	1398974	0.00384	0.08471	0.382	0.000324
Control	160785553	617640	0.00377	0.08332	0.375	0.000313
Control	4752862	18308	0.00385	0.09109	0.383	0.000349
TriplatinNC (20 µM, 1 h)	365604244	1525815	0.00417	0.08112	0.416	0.000337
TriplatinNC (20 µM, 1 h)	1144990	19907	0.00409	0.08479	0.407	0.000345
TriplatinNC (20 µM, 1 h)	579499	9128	0.00412	0.08665	0.411	0.000356
TriplatinNC (20 µM, 2 h)	329763070	1496204	0.00454	0.08194	0.452	0.000370
TriplatinNC (20 µM, 2 h)	952082	14276	0.00434	0.08680	0.432	0.000375
TriplatinNC (20 µM, 2 h)	252888	8252	0.00454	0.10159	0.452	0.000459
TriplatinNC (20 µM, 2 h)	641787	12804	0.00504	0.09636	0.501	0.000483
Cisplatin (20 µM, 1 h)	279357711	1059427	0.00379	0.09734	0.378	0.000368
Cisplatin (20 µM, 1 h)	136924685	520520	0.00382	0.10049	0.381	0.000382
Cisplatin (20 µM, 1 h)	5044008	19358	0.00381	0.12979	0.380	0.000493
Cisplatin (20 µM, 2 h)	270760730	1035808	0.00383	0.09844	0.381	0.000375
Cisplatin (20 µM, 2 h)	126314560	483590	0.00381	0.09606	0.380	0.000365
Cisplatin (20 µM, 2 h)	10665376	40887	0.00381	0.09199	0.380	0.000350

Table S2. $^{15}N/^{14}N$ ratio and ^{15}N enrichment data extracted from three separate secondary ion images for each treatment, for the nucleoli.

Treatment	$^{12}C^{14}N^-$	$^{12}C^{15}N^-$	Ratio	Rel. error (%)	^{15}N (at%)	+/-
Control	4752862	18308	0.00385	0.74047	0.384	0.002841
Control	20320551	76674	0.00377	0.36182	0.376	0.001360
Control	10642337	41005	0.00385	0.49478	0.384	0.001899
TriplatinNC (20 µM, 1 h)	1493739	5863	0.00393	1.30851	0.391	0.005116
TriplatinNC (20 µM, 1 h)	11385290	44128	0.00388	0.47696	0.386	0.001842
TriplatinNC (20 µM, 1 h)	10228515	39890	0.00390	0.50166	0.388	0.001949
TriplatinNC (20 µM, 2 h)	7632003	32211	0.00422	0.55836	0.420	0.002347
TriplatinNC (20 µM, 2 h)	17028263	72413	0.00425	0.37240	0.423	0.001577
TriplatinNC (20 µM, 2 h)	28594256	114958	0.00402	0.29553	0.400	0.001183
Cisplatin (20 µM, 1 h)	5044008	19358	0.00384	0.72011	0.382	0.002753
Cisplatin (20 µM, 1 h)	2870045	11172	0.00389	0.94794	0.388	0.003676
Cisplatin (20 µM, 1 h)	5854322	22266	0.00380	0.67144	0.379	0.002544
Cisplatin (20 µM, 2 h)	10665376	40887	0.00383	0.49549	0.382	0.001892
Cisplatin (20 µM, 2 h)	20069598	76916	0.00383	0.36126	0.382	0.001379
Cisplatin (20 µM, 2 h)	2853479	10886	0.00381	0.96028	0.380	0.003649

Table S3. $^{15}N/^{14}N$ ratio and ^{15}N enrichment data extracted from three separate secondary ion images for each treatment, for the nuclei.

Treatment	$^{12}C^{14}N^-$	$^{12}C^{15}N^-$	Ratio	Rel. error (%)	^{15}N (at%)	+/-
Control	156032690	599331.403	0.00384	0.12942	0.383	0.000493
Control	205697749	775746.666	0.00378	0.11375	0.376	0.000426
Control	123950232	477449.973	0.00385	0.14500	0.384	0.000554
TriplatinNC (20 µM, 1 h)	122547482	474679.581	0.00387	0.14543	0.386	0.000559
TriplatinNC (20 µM, 1 h)	117427420	454690.103	0.00387	0.14859	0.386	0.000571
TriplatinNC (20 µM, 1 h)	114165026	441317.013	0.00387	0.15082	0.385	0.000579
TriplatinNC (20 µM, 2 h)	156077739	618479.844	0.00396	0.1271	0.395	0.000501
TriplatinNC (20 µM, 2 h)	138512806	548982.733	0.00396	0.13523	0.395	0.000532
TriplatinNC (20 µM, 2 h)	66443118.4	260954.228	0.00393	0.19614	0.391	0.000764
Cisplatin (20 µM, 1 h)	131880678	501161.641	0.00380	0.14153	0.379	0.000534
Cisplatin (20 µM, 1 h)	140229871	536482.356	0.00383	0.13679	0.381	0.000519
Cisplatin (20 µM, 1 h)	96660387.9	368754.492	0.00381495	0.16499021	0.380	0.000625
Cisplatin (20 µM, 2 h)	115649184	442702.505	0.00382798	0.15058221	0.381	0.000572
Cisplatin (20 µM, 2 h)	103314304	394119.947	0.00381477	0.15959254	0.380	0.000604
Cisplatin (20 µM, 2 h)	137120197	524039.128	0.00382175	0.1384033	0.381	0.000525

EXPERIMENTAL

Synthesis of ^{15}N-TriplatinNC and ^{15}N-cisplatin

^{15}N-TriplatinNC was prepared as previously reported.[1] *cis*-[$PtCl_2(^{15}NH_3)_2$] was synthesised according to Kerrison and Sadler[2] and recrystallised from aqueous KCl.

Cell culture

MCF7 (human breast adenocarcinoma) cells (American Tissue Culture Collection, Manassas, VA, USA) were cultured in RPMI 1640 Glutamax medium, supplemented with 2mM Glutamax, antibiotics (100 units mL^{-1} Penicillin G sodium, 10 mg mL^{-1} Streptomycin sulphate, 25 mg mL^{-1} Amphotericin B) and foetal bovine serum (all from Invitrogen, Australia), and passaged every 3 – 5 days.

Cell preparation

MCF7 cells were incubated in 3 mL of their growth medium containing ^{15}N-Cisplatin or ^{15}N-TriplatinNC (from a 10 mM stock to a final concentration of 20 µM in the culture flask) for up to 2 h at 37 ºC. After 2 h incubation, the cells were washed twice with phosphate buffered saline (5 mL), before being gently scraped from the culture flask. After centrifugation (5 min at 1200 rpm), the supernatant was discarded, and the cell pellet was gently mixed with a 2% low temperature gelling agarose solution in the culture medium (as a cryoprotectant) in a 1:1 ratio of cell pellet to cryoprotectant, at 37ºC. An aliquot of the cell mixture (1 µL) was transferred to a preheated (37 ºC) flat specimen carrier (gold plated, 0.5 mm think, 1.5 mm cavity diameter, 0.2 mm cavity depth, Leica Microsystems, AG, Wetzler, Germany), and the cells were immediately frozen in the Leica EM PACT2 high-pressure freezer. The carriers with the frozen samples were kept under liquid N_2 until required. When required, the cells in the carriers were transferred into vials containing 100% acetone or an mixture containing acetone + 1% OsO_4 + 0.1% uranyl acetate + 3% H_2O, which was frozen prior using in liquid N_2. The samples were transferred into an automatic freeze-substitution unit pre-cooled to -90ºC. The freeze substitution was carried out over 3.5 days, using the automatic regime of the Leica EM AFS2 machine. After 3.5 days the cells were at 0ºC, and were brought to room temperature over 1 h and the samples were washed in acetone (1 mL), twice. The cell pellets were removed from the gold holders under acetone and carefully transferred to the lid of a small plastic eppendorf tube for embedding. This solution was removed and the samples incubated at room temperature for 4h, overnight, and 2 h, in 50%, 75%, and 100% procure araldite (in acetone), respectively, before being polymerised at 70ºC for 48 h.

NanoSIMS

For NanoSIMS imaging, the cells were prepared and the cell block trimmed as for TEM, however 1 µm sections were cut using a glass knife, placed onto a polished silicon wafer and coated with 20 nm of carbon. NanoSIMS element maps were acquired using the CAMECA NanoSIMS 50 at the University of Western Australia. A Cs^+ primary ion beam with a total impact energy of 16 keV was used for imaging negative secondary ions.

For the imaging of Pt in the cells, the mass spectrometer was tuned to detect $^{12}C^{15}N^-$, $^{31}P^-$, $^{12}C_3^-$ and $^{195}Pt^-$ ions, simultaneously. Pt has several isotopes, with ^{195}Pt the most abundant at 33.8%. The position of the $^{195}Pt^-$ mass peak was calibrated using an embedded and polished piece of Pt metal. A previous study[1] identified an isobaric interference on mass 195 and opted to use the $^{194}Pt^-$ signal (33.0 % abundance), although this was not necessary in this study as the only isobaric interferences were adequately resolved (mass resolving power, $m/\Delta m$ of ~ 6000), and the detector positioned such that none of the isobaric interference contributed to the recorded Pt signal (Fig S8). Furthermore, similar isobaric interferences were also present on mass 194, although the magnitude was twice that of the interfering peaks on mass 195.

As N has an electron affinity of zero and does not ionise directly in SIMS, it is necessary to detect N as a CN^- ion. Due to the physical limitations of the mass spectrometer, it is not possible to detect both $^{12}C^{14}N^-$ and $^{12}C^{15}N^-$ together with $^{195}Pt^-$, therefore for the imaging of $^{15}N/^{14}N$ in the cells, the mass spectrometer was retuned to detect $^{12}C^-$, $^{16}O^-$, $^{12}C^{14}N^-$, $^{12}C^{15}N^-$ and $^{31}P^-$ ions, simultaneously. The position of the $^{12}C^{15}N^-$ peak was calibrated using a graphite planchette doped with a ^{15}N-rich organic solvent, and the mass spectrometer was tuned to resolve the $^{12}C^{15}N^-$ from the $^{13}C^{14}N^-$ peak ($m/\Delta m$ = ~ 10 000, CAMECA definition).

Prior to imaging, each region was implanted with the Cs primary ion beam to a dose of 6 x 10^{16} ions/cm^2. A 300 µm primary aperture was used to achieve a primary beam diameter of ~ 110 nm with a beam current of ~3.5 pA. The beam was rastered over an area of 12 µm x 12 µm, at a resolution of 256 x 256 pixels, with a dwell time of 60 ms/pixel (dwell times were kept constant across all images and samples). The secondary ion signals were recorded using electron multipliers.

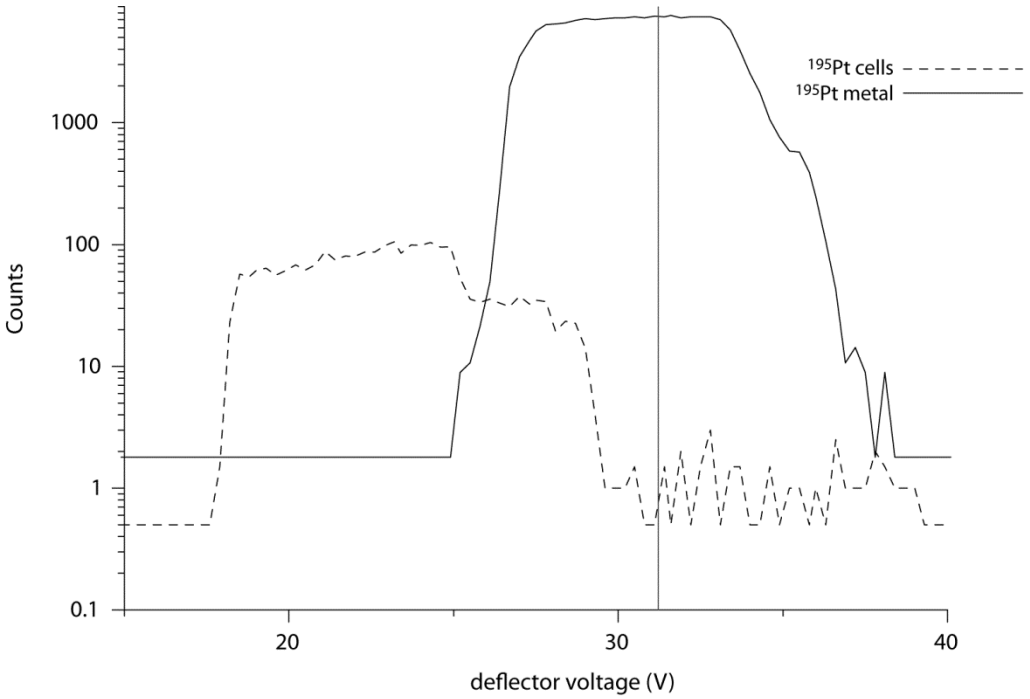

Fig. S8 High-mass-resolution scans of the peaks on mass 195. Deflector plates located before the detector are used to fine-tune the detector to accept only the desired peak. The position of the $^{195}Pt^-$ peak was determined using metallic Pt foil, and the deflectors were adjusted slightly to avoid an unknown isobaric interference present in the sample.

Image processing and data extraction

All NanoSIMS image processing was performed using ImageJ (W.S. Rasband, ImageJ, US National Institutes of Health, Bethesda, MD, USA, http://rsb.info.nih.gov.ij/, 1997–2006) in conjunction with the OpenMIMS plugin (National Resource for Imaging Mass Spectrometry, http://www.nrims.hms.harvard.edu). Data consist of 32-bit image files, recording the raw ion counts and x-y location for each pixel. All images were corrected pixel-by-pixel for 44 ns detector deadtime prior to any other processing function. All image processing was performed on the 32-bit data files, without any conversion to any other format. N ratio images were obtained by dividing the $^{12}C^{15}N^-$ ion image by the $^{12}C^{14}N^-$ ion image, using a ratio scale factor of 10,000, and setting the upper and lower limits to 36 (to reflect the natural isotopic abundance of 0.00365) and 72, respectively. ^{15}N enrichment is expressed as a hue-saturation-intensity image (HSI), where the colour scale represents the $^{15}N/^{14}N$, and the intensity an index of the statistical reliability. [2] The colour scale is based on the same upper and lower limits as the ratio image – ie, the dark blue on the left represents natural isotopic abundance, while a shift in colour to the right indicates enrichment in ^{15}N up to 0.0072. This method allows very small variations in the ratio to be displayed with more clarity than the ratio images.

Despite the fact that both sets of secondary ion images were acquired from the same physical coordinates, there was some drift during the acquisition, which means that it is not possible to directly align the $^{15}N/^{14}N$ image with ^{195}Pt image. But as the $^{12}C^{15}N^-$ image was acquired simultaneously with the ^{195}Pt signal, it is possible to overlay these images to directly compare the colocalisation.

The $^{15}N/^{14}N$ ratio and ^{15}N-enrichment data presented in tables S1, S2 and S3 were obtained from the deadtime-corrected images by drawing regions of interest (ROI) and extracting the total ions counts within each ROI. Different ROIs were used, ranging from the whole cell to the nucleolus and individual ^{15}N hotspots (the enrichment in the nucleus was determined by subtracting the value for the nucleolus). Analytical uncertainties are based on the Poisson counting statistics for the total number of secondary ions recorded within each ROI, using the expression:

$$= \sqrt{\frac{1}{N_1} + \frac{1}{N_2}}$$

where N_1 and N_2 are the number of ion counts recorded for each secondary ion species (ie, $^{12}C^{15}N^-$ and $^{12}C^{14}N^-$), respectively.
The ^{15}N enrichment (in atom%) is calculated by

$$\frac{^{15}N}{(^{15}N+^{14}N)} \times 100$$

and the uncertainty is similarly an estimation based on the counting statistics. The standard error of the mean (SE) of the control cells is 0.66%, indicating that the error associated with the reproducibility of the measurements is somewhat larger than the analytical uncertainty, although with an *n* of only 3, it is difficult to fully assess. Assuming the controls have no ^{15}N enrichment, the instrumental mass fractionation is approximately 0.045, using the expression:

$$\mathrm{IMF} = \left(\frac{\frac{R_{control}}{R_{natural}} - 1}{\Delta m} \right)$$

where $R_{control}$ is the mean ratio for the three control cells (0.00382), $R_{natural}$ is the natural isotopic abundance ratio (0.00365), and Δm is the difference in mass between ^{14}N and ^{15}N.

References

1. Y. Qu, A. Harris, A. Hegmans, A. Petz, P. Kabolizadeh, H. Penazova and N. Farrell, *J. Inorg. Biochem.*, 2004, **98**, 1591-1598.
2. S. J. S. Kerrison and P. J. Sadler, *J. Chem. Soc. Chem. Comm.*, 1977, 861-863.